


Low eigenvalues of the entanglement Hamiltonian, localization length, and rare regions in one-dimensional disordered interacting systems

Richard Berkovits

Department of Physics, Jack and Pearl Resnick Institute, Bar-Ilan University, Ramat-Gan 52900, Israel
 (Received 10 October 2017; revised manuscript received 4 February 2018; published 8 March 2018)

The properties of the low-lying eigenvalues of the entanglement Hamiltonian and their relation to the localization length of a disordered interacting one-dimensional many-particle system are studied. The average of the first entanglement Hamiltonian level spacing is proportional to the ground-state localization length and shows the same dependence on the disorder and interaction strength as the localization length. This is the result of the fact that entanglement is limited to distances of order of the localization length. The distribution of the first entanglement level spacing shows a Gaussian-type behavior as expected for level spacings much larger than the disorder broadening. For weakly disordered systems (localization length larger than sample length), the distribution shows an additional peak at low-level spacings. This stems from rare regions in some samples which exhibit metalliclike behavior of large entanglement and large particle-number fluctuations. These intermediate microemulsion metallic regions embedded in the insulating phase are discussed.

DOI: [10.1103/PhysRevB.97.115408](https://doi.org/10.1103/PhysRevB.97.115408)

I. INTRODUCTION

Close to 60 years after the concept of localization has been introduced by Anderson [1], the localization transition remains at the center of many current topics, from applications of many body in quantum information [2] to random lasing [3]. While for most quantum phases the gap between the ground-state energy and the first excited state defines the correlation length, in the localized phase the correlation length corresponds to the localization length, determined by the exponential dependence of the conductance G on the linear dimension of the system L . The localization length ξ is defined through the exponential decrease in the conductance in the localized phase $G(L) \sim \exp(-L/\xi)$ [4].

It is important to note that when one discusses the localization of disordered one-dimensional (1D) electrons, one must differentiate between noninteracting and interacting electrons, and between states close to the ground state and highly excited states. For noninteracting electrons, all states are localized whether they are in the vicinity of the ground state or highly excited. On the other hand, for interacting electrons, states close to the ground state are *always* localized, while highly excited states are delocalized. This localization-delocalization transition is known as the many-body localization (MBL) transition and may occur at a given excitation energy for a specific interaction strength [5,6].

Recently, it was realized that ξ should also determine the entanglement properties of a system in the strongly localized regime [7]. One does not expect regions beyond the distance ξ to be entangled. Thus, by dividing a one-dimensional system into two regions (see Fig. 1), and studying the entanglement between them, one may hope to gain a measure of ξ through the entanglement properties. Indeed, for the ground state, the averaged entanglement entropy increases logarithmically as long as the length of region A , L_A , is smaller than than ξ and saturates for $L_A > \xi$ [7,8]. For excited states, where the

entanglement entropy is expected to follow the volume law, one expects the averaged entanglement entropy to increase as L_A for $L_A < \xi$, and saturate for longer length [9]. Here, we would like to use ground-state entanglement as a window into the physics of the region within length ξ from the boundary. As long as the system is in the localized regime (i.e., finite ξ) similar methods should work also for excited states.

The information regarding the entanglement between the regions A and B is encoded in the reduced density matrix (RDM), $\rho_{A(B)}$, of regions A (or B). For a system in a pure state $|\Psi\rangle$, ρ_A is defined as $\rho_A = \text{Tr}_B |\Psi\rangle\langle\Psi|$, where the degrees of freedom of region B are traced out. It is important to note that diagonalizing ρ_A defines a basis that completely spans the Hilbert space of region A and if there exists any conserved quantum number (for the case discussed in this paper the conserved quantum number is N_A , the number of particles in region A), that basis is also the eigenvector of N_A . The eigenvalues of the RDM, $\lambda_i^{N_A}$, are used to extract measures for the entanglement between the regions, such as the entanglement entropy, defined as $S_A = -\sum_i \lambda_i^{N_A} \ln \lambda_i^{N_A}$, and the Rényi entropy $S_{nA} = -\frac{1}{1-n} \ln \sum_i (\lambda_i^{N_A})^n$, where the first Rényi entropy ($n \rightarrow 1$) is equal to the entanglement entropy.

Recently, Li and Haldane [10] have suggested a different way to interpret the eigenvalues of the RDM. They noted that the RDM of region A may be seen as a density matrix of a mixed thermal state of an ersatz system described by a Hamiltonian H_A such that $\rho_A = \exp(-\beta H_A)$, where H_A is known as the entanglement Hamiltonian and $\beta = 1$. Under these conditions, the eigenvalues of H_A are given by $\varepsilon_i^{N_A} = -\ln(\lambda_i^{N_A})$. Up until now, these are just mathematical manipulations, but Li and Haldane noted that for a fractional quantum Hall $\nu = \frac{5}{2}$ state where the bulk is partitioned into two regions and a virtual edge is created, the eigenvalues $\varepsilon_i^{N_A}$ resembled the true edge excitation spectrum. This is actually quite intuitive since the boundary between regions A and B is the edge and therefore

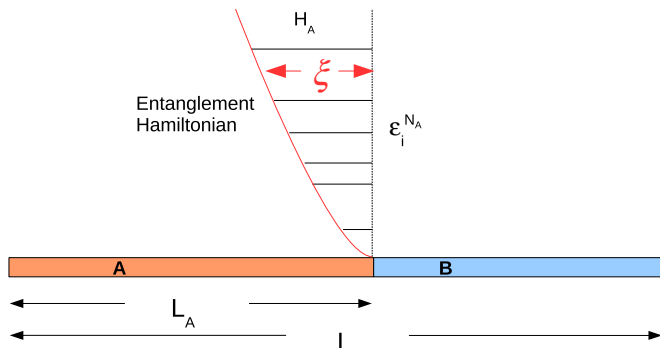


FIG. 1. A schematic representation of the system and the entanglement Hamiltonian H_A . A one-dimensional system of length L is bisected into two regions A and B , with length L_A and $L - L_A$. The reduced density matrix of region A , ρ_A , is calculated and its eigenvalues $\lambda_i^{N_A}$ are used to construct the entanglement Hamiltonian H_A and its eigenvalues $\epsilon_i^{N_A}$. H_A samples the behavior of the system on a scale ξ from the A - B boundary.

one should expect H_A to give a reasonable representation of the physics of the edge. This suggests that the low-energy entanglement Hamiltonian spectrum shows some correspondence to the true many-body excitations close to partition (the edge region). This correspondence has been demonstrated for different cases of topological insulators [11,12].

The situation for the entanglement between regions A and B for a 1D system depicted in Fig. 1 where the contact between the two regions is a point. As pointed out by Alba *et al.* [13], for different 1D gapped systems (i.e., systems with finite correlation length) one expects that the entanglement spectrum will be mainly influenced by a region of order of the correlation length from the boundary. This is similar to the situation in the Anderson localized phase, where there is no gap but the localization length plays the role of a correlation length [4]. This is highlighted by the saturation of the entanglement entropy once $L_A > \xi$ discussed earlier, as well as by power-law behavior which depends on the localization length of the entanglement spectrum of a highly excited state [14] in the many-body localized regime.

In this paper, we show that the entanglement spectrum of the ground and low-lying excitation states of a localized interacting 1D many-particle system shows a clear signature of the many-particle localization length. Specifically, the first level spacing of the entanglement energies for a given N_A , $\Delta_1^{N_A} = \epsilon_2^{N_A} - \epsilon_1^{N_A}$, is proportional to $1/\sqrt{\xi}$. As we shall explain, this is the behavior expected from a many-particle state trapped in a potential of width ξ from the boundary. Moreover, the proportionality depends linearly on the strength of particle-particle interactions U as expected from charge particles trapped in a potential. It is also shown that deep in the localized regime, where no difference in the localization length between the many-particle ground state and the low-lying states is expected, also $\Delta_1^{N_A}$ is similar. On the other hand, for weaker disorder, where the localization length for low-lying excitations is significantly larger than for the ground state [9], also $\Delta_1^{N_A}$ becomes smaller. The distribution of $\Delta_1^{N_A}$ becomes Gaussian for $\xi \ll L_A$, with a width proportional to disorder

and does not depend on U , as might be expected for the level spacing of states in a weakly disordered quantum dot.

This is important not only as a new simple way of determining the localization length of an interacting many-particle system, but mainly as a way to access the properties of disordered many-particle systems on short length scales (of scale ξ) and large energy scales $U/\sqrt{\xi}$. This is illustrated by using the low-lying values of ϵ to detect and characterize rare regions in the sample which appear for low-disorder strongly interacting samples. These regions exhibit metalliclike behavior such as large entanglement and high particle-number variance.

The paper is organized as follows: In Sec. II the model for the interacting fermions in a disordered one-dimensional system is defined. The next section (Sec. III) discusses the average of the first entanglement level spacing and its relation to the ground-state localization length. The following section (Sec. IV) investigates the properties of the distribution of the first entanglement level spacing. The appearance of some rare regions in the sample which exhibit metalliclike features is discussed in Sec. V. The significance of the results and relevance to further work is discussed in Sec. VI.

II. MODEL

In this paper, we study spinless electrons confined to a 1D wire of length L with repulsive nearest-neighbor particle-particle interactions and onsite disordered potential, depicted by the Hamiltonian

$$H = \sum_{j=1}^L \epsilon_j \hat{c}_j^\dagger \hat{c}_j - t \sum_{j=1}^{L-1} (\hat{c}_j^\dagger \hat{c}_{j+1} + \text{H.c.}) + U \sum_{j=1}^{L-1} \left(\hat{c}_j^\dagger \hat{c}_j - \frac{1}{2} \right) \left(\hat{c}_{j+1}^\dagger \hat{c}_{j+1} - \frac{1}{2} \right), \quad (1)$$

in which ϵ_j represents the onsite energy drawn from a uniform distribution $[-W/2, W/2]$, \hat{c}_j^\dagger is the creation operator of a spinless particle at site j , and $t = 1$ is the hopping matrix element. The interaction strength is U , with a background positive charge. For this model the localization length $\xi_0 \approx 105/W^2$ [15] for $U = 0$. The Luttinger parameter is defined as $K(U) = \pi/[2 \cos^{-1}(-U/2)]$ [16,17], where $K(U = 0) = 1$. As U increases, K becomes smaller, and at the transition to a charge density wave ($U = 2$) $K = \frac{1}{2}$. Renormalization group scaling of the localization length suggests $\xi = (\xi_0)^{1/(3-2K)}$ [18,19], i.e., ξ decreases as the interaction increases and the system becomes more localized.

III. AVERAGED FIRST ENTANGLEMENT LEVEL SPACING

We use the numerical density matrix renormalization group (DMRG) [20,21] method to calculate the RDM for the ground state and low-lying excited states of the Hamiltonian depicted in Eq. (1) [7,9] at half-filling. We calculate the eigenvalues of the RDM for a system of length $L = 700$, different values of disorder $W = 0.3, 0.7, 1.5, 2.5, 3.5, 4, 5$ corresponding to $\xi \sim 1100, 200, 50, 20, 9, 6.5, 4$, different values of interaction strength $U = 0, 0.3, 0.6, 0.9, 1.2, 1.5, 1.8, 2.1, 2.4$ corresponding to $K = 1, 0.91, 0.84, 0.77, 0.71, 0.65, 0.58, 0.49, 0.48$

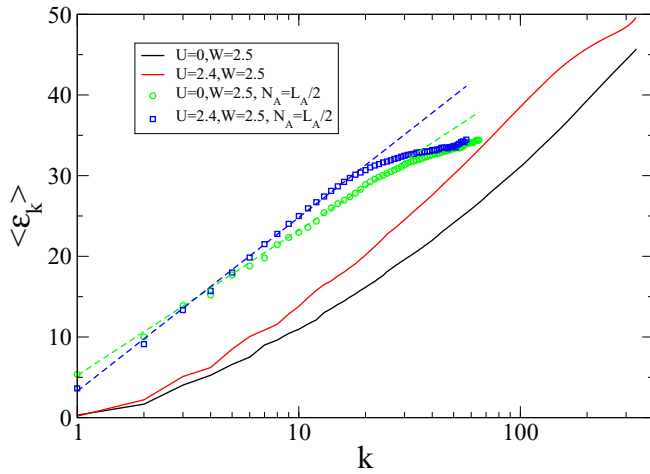


FIG. 2. The averaged entanglement Hamiltonian levels $\langle \varepsilon_k \rangle$ (lines) and averaged entanglement levels for a fixed number of particles in region A ($\varepsilon_k^{N_A=L_A/2}$) (symbols) as function of the level number k for a system of size $L = 700$ where $W = 2.5$ and $U = 0, 2.4$. For both noninteracting and interacting cases, $\langle \varepsilon_k \rangle$ increases stronger than a power law, while $\langle \varepsilon_k^{N_A=L_A/2} \rangle$ follows a power law (indicated by a dashed line), for low values of k .

(the two last values are a continuation of the values K for $U = 2$) and different sizes of region A : usually, $L_A = 10, 20, \dots, L - 10$, for at least 100 realizations of onsite disorder.

Here, we concentrate on the first level spacing of the entanglement levels, but prior to addressing this quantity it is informative to consider the behavior of the low-lying entanglement spectrum. Since the number of electrons in region A remains a good quantum number of H_A , for each eigenstate of ρ_A one should calculate both λ_i and N_i^A (the number of particles in the region A). Calculating N_i^A does not add to the complexity of the DMRG code [22]. The averaged entanglement Hamiltonian eigenvalue $\langle \varepsilon_k \rangle$ (where $\langle \dots \rangle$ depicts an average over different realization of disorder and values of L_A in the vicinity of $L/2$) and the averaged entanglement Hamiltonian eigenvalue for a particular value of N_A , $\langle \varepsilon_k^{N_A=L_A/2} \rangle$, are plotted in Fig. 2, for a relative strong disorder $W = 2.5$ and two values of interaction $U = 0, 2.4$. For the entanglement spectrum of highly excited states of small systems in the many-body localized regime, it has been shown that $\langle \varepsilon_k \rangle$ as function of k behaves as a power law [14]. Here, the entanglement spectrum of the ground state in the localized regime $\langle \varepsilon_k \rangle$ rises faster than a power law, but when one takes only the entanglement spectrum belonging to the same sector N^A one discovers that the low-lying spectrum indeed follows a power law until it saturates.

Next, the average first level spacing $\Delta_1^{N_A}(L_A) = \langle \varepsilon_2^{N_A}(L_A) - \varepsilon_1^{N_A}(L_A) \rangle$ is calculated. It is important to note that as for the entire low-lying spectrum, if one ignores the subscript N_A and calculates $\varepsilon_2 - \varepsilon_1$ one gets a very different result. Essentially, since eigenstates of ρ_A belonging to different sectors of N_A do not couple, one obtains a spacing of two unrelated energies which does not contain much physical information. On the other hand, $\Delta_1^{N_A}$ does not depend strongly on N_A and therefore we also average over values of $N_A \sim L_A/2$ to obtain Δ_1 .

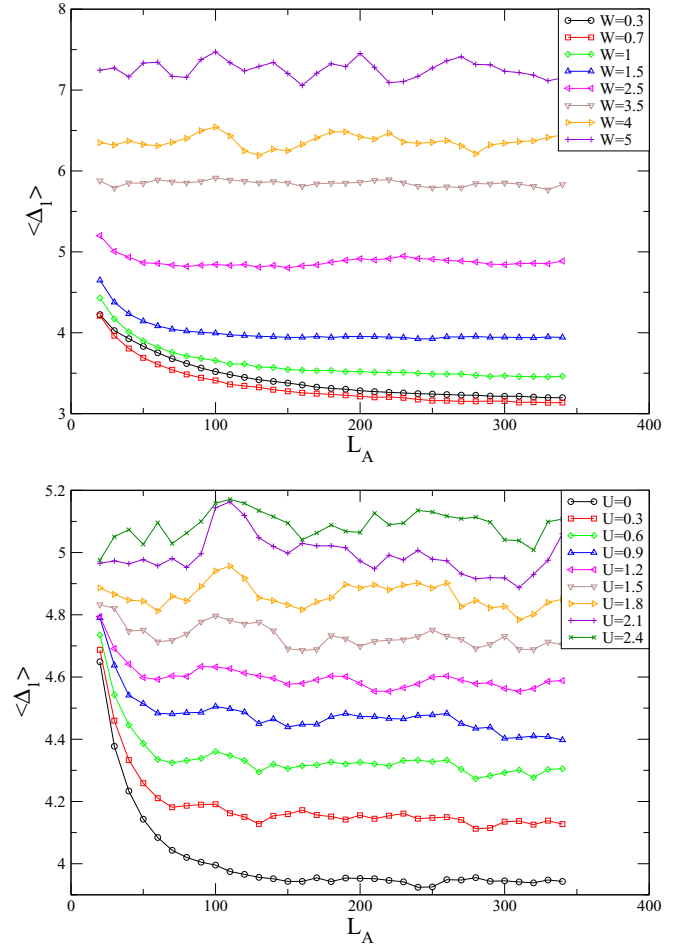


FIG. 3. The averaged first level spacing Δ_1 as function of the size of region A , L_A , for a system of size $L = 700$ and different values of disorder W or interaction strength U . Top: the noninteracting case for different values of W . Bottom: for $W = 1.5$ ($\xi_0 = 50$) and different values of U . In both cases, it is clear that as ξ decreases whether due to increasing disorder or interaction strength, Δ_1 saturates at smaller values of L_A , indicating a finite region in A influenced by the entanglement.

In Fig. 3, $\Delta_1(L_A)$ for different values of disorder W and interaction strength U are presented. Since we expect that there will be no entanglement beyond a region proportional to ξ , the entanglement spectrum should be affected by the shortest length scale of L_A or ξ . Thus, $\Delta_1(L_A > \xi) = \Delta_1(\xi)$ should saturate, which is indeed seen for higher values of W and U for which ξ becomes shorter. Another feature of $\Delta_1(L_A)$ which should be considered is its magnitude. A simple consideration, treating the fact that the entanglement is confined to the boundary between the regions as an effective confining potential of width ξ in H_A (see Fig 1), will result in $\Delta_1(\xi) \propto 1/\xi$. This argument neglects the fact that we are calculating the level spacing within the same sector N_A . Thus, one must consider that the next state might not belong to the same N_A sector. Taking into account that the variance in the number of particles in region A is proportional to $\sqrt{\xi}$, one concludes that $\Delta_1(\xi) \propto 1/\sqrt{\xi}$.

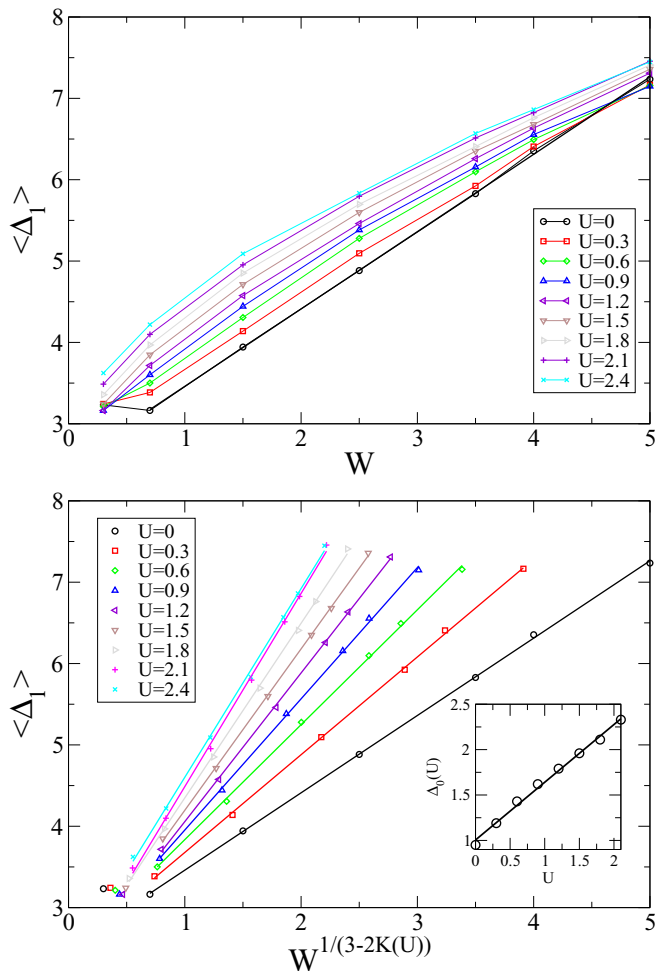


FIG. 4. The averaged first level spacing Δ_1 as function of the disorder W and interaction strength U averaged also over the central region on the wire $L/4 < L_A < 3L_A/4$ (symbols). Top: Δ_1 as function of the disorder strength. For the noninteracting case ($U = 0$), as long as $\xi < L$ (i.e., as long as $W > 0.5$) Δ_1 is linearly dependent on W (black line), in line with the expectation from $\Delta_1 \propto 1/\sqrt{\xi_0}$. This relation does not hold for the interacting case $U > 0$. Bottom: taking into account the influence of U on the localization length. Here, we plot Δ_1 as function of $1/\sqrt{\xi} \propto W^{1/(3-2K(U))}$. A linear dependence on $1/\sqrt{\xi}$ with a slope depending on interaction $\Delta_0(U)$ is clear (lines). As expected from interacting particles in a confining potential $\Delta_0(U) \propto U$, as can be seen in the inset.

This behavior is seen in Fig. 4 where Δ_1 for different values of disorder and interaction are indicated by the symbols. Since (except for $W = 0.3$) in all cases $\xi \leq 200$ we have also averaged over the different values of L_A in the range $L/4 < L_A < 3L_A/4$, where the first level spacing saturates. In the top figure, Δ_1 is plotted as function of $1/\sqrt{\xi_0} \propto W$. As indicated by the black line, for the noninteracting case ($U = 0$), as long as $\xi < L$ (i.e., $W > 0.4$) the numerical data follow $1/\sqrt{\xi_0}$ perfectly. For the interacting cases, deviations are clearly seen. That is not surprising since ξ depends on U . Taking the dependence of the localization length on the interactions into account by $1/\sqrt{\xi} \propto W^{1/(3-2K(U))}$, a linear relation of the form $\Delta_1 = \Delta_0(U)/\sqrt{\xi} + \text{const}$ can be seen in the lower panel of Fig. 4. Moreover, as can be seen in the

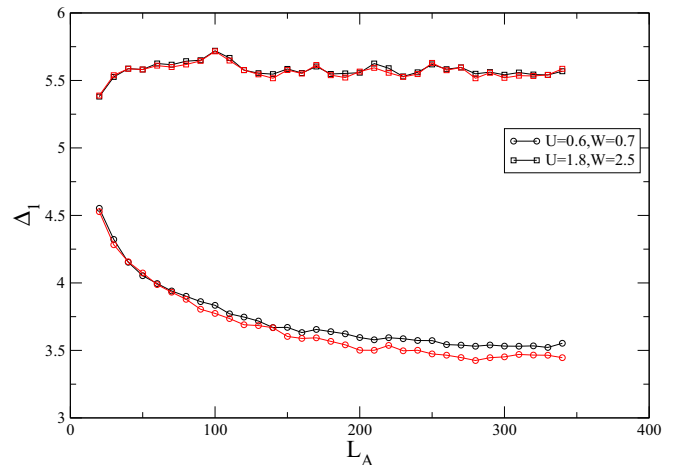


FIG. 5. Comparison of the averaged first entanglement level spacing between the ground state (black) and the first excited state (red). For the strongly localized case $U = 1.8, W = 2.5$ there is no difference between the two. On the other hand, for the weak disorder case $U = 0.6, W = 0.7$, Δ_1 is consistently lower in the saturated region for the excited state.

inset, $\Delta_0(U)$ depends linearly on U as may be expected from the level spacing of charged particles in a confined potential (Coulomb blockade) [23]. This further strengthens the picture of the entanglement spectrum corresponding to a many-particle spectrum of an effective Hamiltonian with a confining potential near the boundary.

Up to now we have considered the case for which the pure state $|\Psi\rangle$ of the entire system is the ground state. Of course, in principle, one may calculate the entanglement spectrum of the system for any pure state. Nevertheless, DMRG is suitable only for the calculation of states for which the entanglement does not grow too much. For long one-dimensional systems, this demand could be fulfilled by the ground state that grows only logarithmically with length, and by excited states in the MBL localized regime, as long as the localization length is short enough (since their entanglement grows linearly up to the localization length) [14,24,25]. Here, we would like to see the influence of ξ for long systems, where ξ spans the whole range from $\xi > L$ to $L \gg \xi$, and therefore we have calculated only the entanglement spectrum for the ground state. In the strong disorder regime, no physical difference is expected between the ground state and the low-lying excitations. Indeed, comparing Δ_1 for the ground state and the first excited state for $U = 1.8, W = 2.5$ (Fig. 5), no significant difference can be seen. On the other hand, for weak disorder it has been shown that even for low-lying excitations there may be a significant increase in the localization length [9]. This can be seen for the weak disorder case of $U = 0.6, W = 0.7$, as a decrease in Δ_1 for the saturated area, as expected when ξ increases.

IV. FIRST ENTANGLEMENT LEVEL SPACING DISTRIBUTION

One might naively expect that the distribution of the first entanglement level spacing will be similar to the first excitation of a localized many-particle system, which should follow

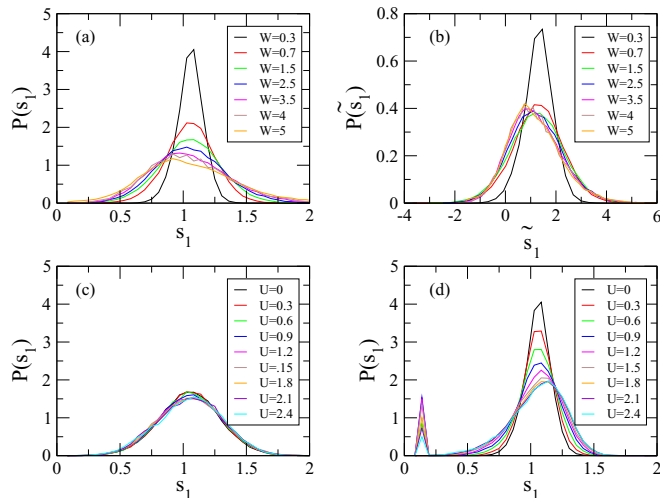


FIG. 6. The numerical distribution of the normalized first entanglement level spacing s_1 for different strength of disorder W and interaction strength U . (a) The distribution for different strength of disorder in the noninteracting ($U = 0$) case. (b) As in (a) where s_1 is rescaled according to $\tilde{s}_1 = (s_1 - 1)(a + bW) + 1$ and $P(\tilde{s}_1) = (a + bW)^{-1}$ where a and b are constants. (c) The distribution for different strength of interaction strength at a given value of disorder $W = 1.5$, the distribution is almost independent of U . (d) As in (c), for weaker disorder $W = 0.7$. In this case, as U increases a second peak in the distribution for small spacings appears.

the single-particle level spacing distribution, i.e., the Poisson distribution [26]. It is also known that the distribution across all the ES level spacings for highly excited states follows a semi-Poisson distribution in the localized regime [27]. The distribution of the normalized first excitation $P(s_1)$ [where $s_1 = (\varepsilon_2^{N_A} - \varepsilon_1^{N_A})/\Delta_1^{N_A}$] is drawn from different realizations of disorder, different cuts of L_A in the range $L/4 < L_A < 3L/4$ and values of $N_A \sim L_A/2$ and presented in Fig. 6(a) for the noninteracting ($U = 0$) case. It is immediately clear that this is not a Poisson distribution, but rather a Gaussian-type broadening of the spacing as function of W . This nonuniversal behavior of the distribution is due to the effective confining potential of the entanglement Hamiltonian. Since only an area of length ξ is sampled by the entanglement spectrum, the system on this length scale is not localized. As is known for disordered 1D systems, the distribution of single-particle level spacing crosses over very rapidly from a universal Poisson distribution when ξ is smaller than the length to a nonuniversal broadening as ξ becomes larger than the systems length, with no true Wigner behavior in the middle [28]. Thus, $P(s_1)$ shows the typical behavior of a short disordered 1D system. The broadening of the distribution is proportional to W , and the distribution might be rescaled by $\tilde{s}_1 = (s_1 - 1)(a + bW) + 1$ and $P(\tilde{s}_1) = (a + bW)^{-1}$ with the numerical factors $a = 0.17$, $b = 0.0375$. As can be seen in Fig. 6(b) after rescaling the curves with stronger disorder ($W > 0.7$) for which the localization length is significantly shorter than the system size, all curves fall on each other.

In the region where $\xi \ll L$ there is no dependence on U as is demonstrated in Fig. 6(c) for the case of $W = 1.5$. Thus, in contrast with the average first level spacing which depends on

ξ , the distribution width depends only on the onsite disorder W and not on U or ξ . Nevertheless, for weak disorder ($W = 0.7$, $\xi \geq L$) a peculiar dependence on U appears. As is seen in Fig. 6(d), a second peak in the distribution at low values of s_1 appears. This peak has a nonmonotonic behavior as function of U . It is absent for $U = 0$ and appears only for stronger values of U . This feature is absent from stronger disordered samples [see Fig. 6(c)].

V. INTERMEDIATE REGIONS IN WEAKLY DISORDERED STRONGLY INTERACTING REALIZATIONS

From where does this second peak for weakly disordered strongly interacting systems come from? Some insight may be gained from scrutinizing specific realizations of disorder. Four representative realizations with ($W = 0.7$, $U = 2.4$) are shown in Fig. 7. For typical regions of each sample s_1 fluctuates around the average and is significantly higher than for a clean case with the same interaction strength ($W = 0$, $U = 2.4$). Nevertheless, there are rare regions (see, e.g., the lowest panel of Fig. 7 in the region $370 < L_A < 470$) where s_1 is significantly lower than the average and much closer to the clean case value. Moreover, the entanglement entropy S_A is strongly enhanced in that region even beyond the clean sample value. Likewise, the particle-number variance $\delta^2 N_A = \langle N_A^2 \rangle - \langle N_A \rangle^2$ (easily calculated using DMRG) is also enhanced in this region, much beyond the values for a clean system ($W = 0$) with the same interaction strength. The correspondence between S_A and $\delta^2 N_A$ seems to work well for these realizations although, strictly speaking, there is no theoretical proof for this relation in interacting systems [22,29,30]. This will be further discussed elsewhere. Anyway, the behavior of both S_A and $\delta^2 N_A$ are in line with a “metallic” inclusion within the localized sample. Thus, although as we have seen for Δ_1 , on the average stronger interactions (U) correspond to

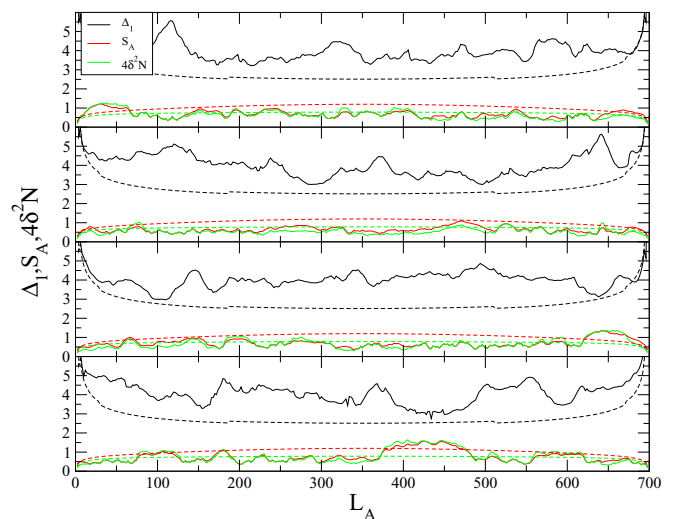


FIG. 7. The first entanglement level spacing s_1 (black curve), the entanglement entropy S_A (red curve), and the particle-number variance $\delta^2 N_A$ (green curve multiplied by 4 for clarity) for four different realizations of disorder, where $W = 0.7$ and $U = 2.4$ and $L_A = 2, 4, 6, \dots, L - 2$. The results for a clean system ($W = 0$, $U = 2.4$) are presented by the corresponding dashed curves.

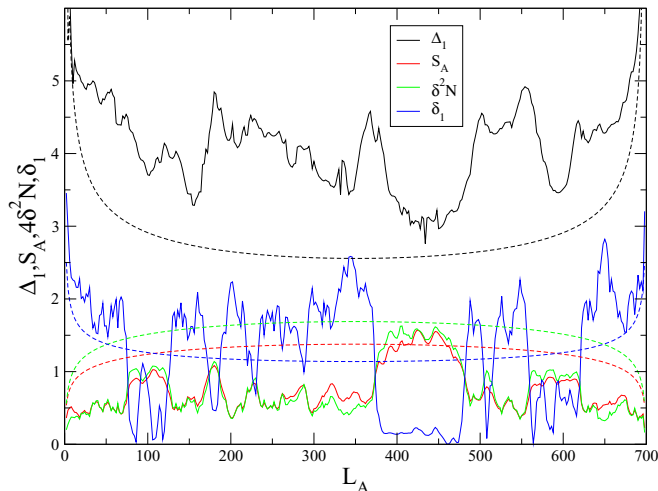


FIG. 8. A closer look at the behavior of the last realization depicted in Fig. 7. The first entanglement level spacing s_1 (black curve), the entanglement entropy S_A (red curve), the particle-number variance $\delta^2 N_A$ (green curve multiplied by 4 for clarity), and the spacing between two lowest entropy levels belonging to different particle number δ_1 (blue curve). For comparison, the same variables calculated for a clean noninteracting sample ($U = 0$, $W = 0$) are indicated by dashed curves.

stronger localization (smaller ξ), there exist rare regions for which the interplay between interaction and disorder may lead to a more metalliclike behavior. A similar behavior, where interactions lead to delocalization in rare realizations of 1D disordered systems, was seen for the persistent current [31], and is also reminiscent of the intermediate microemulsion phases proposed for two-dimensional systems [32].

Some light on the nature of these rare regions can be shed by the low-lying entropy energies $\varepsilon_i^{N_A}$. Usually, for the half-filled case discussed here, and an even partition (L_A even), $\varepsilon_1^{N_A=L_A/2}$ is much lower than any other energy since a state with $N_A = L_A/2$ is the most probable. Thus, one expects $\delta_1 = \min(\varepsilon^{(N_A=L_A/2 \pm 1)} - \varepsilon_1^{N_A=L_A/2})$ to be smaller than Δ_1 , but not orders of magnitude lower. Indeed, comparing δ_1 to Δ_1 for the last realization depicted in Fig. 7 (see Fig. 8) shows this behavior for most of the sample, except for the region around $370 < L_A < 470$, and smaller regions around $L_A = 100$ and $L_A = 600$ where δ_1 reaches values close to zero. These are exactly the regions where strongly enhanced values of S_A and $\delta^2 N_A$ are seen, i.e., close to the values of a metallic sample ($U = 0$, $W = 0$). For typical regions of the strongly interacting weakly disordered system, the ground state is a pinned charge density wave leading to small variance in the number of particles and low entanglement entropy. In contrast, the rare regions are neither described by a charge density wave nor by a simple metallic behavior. This can be clearly seen from the very different behavior of δ_1 in these regions compared to regular metals. As seen in Fig. 8, especially for the region around $370 < L_A < 470$, δ_1 is much lower for the disordered rare region than for a clean system. This indicates that these rare regions are governed by different physics than the usual metallic 1D system. The fact that $\delta_1 \sim 1$ indicates large and almost equal contribution to the many-particle state

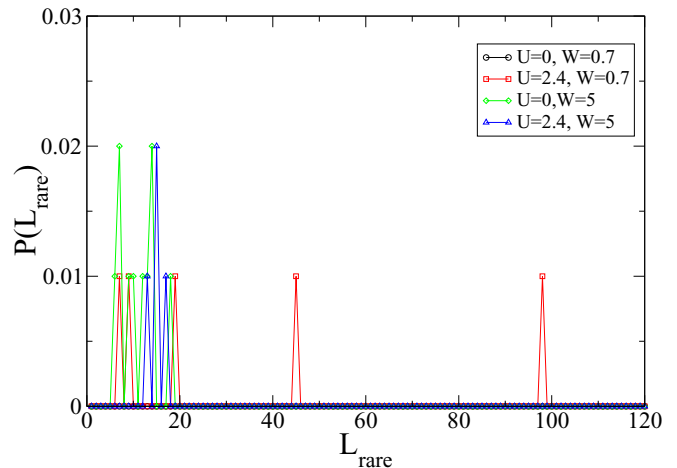


FIG. 9. The probability of finding a rare metallic region of length L_{rare} where such a region is defined as a consecutive region, of length larger than 5, for which $\delta_1 < 0.3$ and $S_A > 1.3\langle S_A \rangle$, for weak ($W = 0.7$) and strong ($W = 5$) disorder and for both noninteracting ($U = 0$) and strongly interacting ($U = 2.4$) cases. For weakly disordered noninteracting systems ($W = 0.7$, $U = 0$), no rare regions were observed in an ensemble of 100 realizations of length $L = 700$. For strong disorder $W = 5$, only short regions $L_{\text{rare}} < 20$ are unfrequently seen, with or without interaction. For weakly disordered strongly interacting systems, one does rarely encounter long ($L_{\text{rare}} \gg 20$) metallic region.

from sectors with different number of particles in region A , which is very different than for the clean metallic situation.

How rare are these rare regions and how does the answer depend on the system's parameters? First, one must take into account that obtaining reliable statistics on rare regions would require a huge number of samples, which is much beyond our current number of realizations. Thus, all we can do with the size of our ensemble is to get some qualitative results regarding these rare regions. In Fig. 9 the probability of finding a rare region of length L_{rare} is plotted for different strength of disorder and interaction. The length L_{rare} is defined as the number of consecutive sites for which δ_1 is much lower than its typical value (i.e., $\delta_1 < 0.3$) and the entanglement entropy is larger than the average ($S_A > 1.3\langle S_A \rangle$). As can be seen in Fig. 9, where the probability of finding such a metallic region for an ensemble of 100 realizations of disorder is depicted, no such regions are seen for the weakly disordered noninteracting systems ($W = 0.7$, $U = 0$). For strong disorder ($W = 5$) there exist a small number of such regions, but they are short, $L_{\text{rare}} < 20$, and do not seem to depend much on the interaction strength. In a sense, the appearance of small regions with “metallic” behavior for strong disorder is not surprising since they can be ascribed to rare local configurations of disorder. The real surprise comes from the detection of a couple of long regions with “metallic” behavior for weakly disordered, strongly interacting systems ($W = 0.7$, $U = 2.4$). The length of these regions $L_{\text{rare}} = 45$ and 98 is surprising since they are significantly longer than the localization length $\xi(W = 0.7, U = 2.4) \sim 14$. Thus, it seems that these rare regions are unique to the weakly disordered strongly interacting regime. One must add a strong cautionary note:

The number of realizations is too small to establish any firm conclusion on the probability of these rare regions and one should increase the ensemble of disorder realizations by at least an order of magnitude.

It is interesting to note that somewhat similar rare regions have been recently discussed in the context of the possibility of Griffiths regions within the many-body localized regime close to the delocalization transition [33,34]. In that context, rare metalliclike (anomalously large localization length) regions act as a thermalizing bath for their insulating surroundings. These regions exist only for interacting systems. Of course, the physics of thermalization is relevant only for highly excited states which have a huge density of states, but as can be seen from our study, metalliclike rare regions seem to appear also for the ground state as long as the disorder is weak, and may have the same origin.

VI. DISCUSSION

Thus, the average of the first entanglement level spacing has been shown to have a clear relation to the ground-state localization length and shows the expected behavior as function of the strength of the onsite disorder and with the repulsive particle-particle interactions. This stems from the fact that for a strongly localized system, the entanglement is confined to a distance of order of the localization length from the boundary between the regions, and that has a clear imprint on the low-lying eigenvalues of the RDM and the corresponding values of the entanglement Hamiltonian. The distribution of the first entanglement level spacing once the localization length

is shorter than the sample length is Gaussian type and quite universal. The distribution depends only on the strength of disorder and not on the interactions. Such a behavior is actually expected for the distribution of low-lying level spacings in a disordered confining potential, as long as the level spacing is larger than the influence of the disorder.

On the other hand, for weakly disordered systems and strongly interacting systems, the distribution shows an interesting peak, signifying an increased probability for almost degenerate level spacings. On closer examination of the behavior for specific realization it becomes clear this feature is connected to rare regions in the sample which exhibit metalliclike behavior. These rare regions in the ground state are composed of more or less equal significant contributions from two states with different number of particles. This not only leaves a distinct signature in the entanglement spectrum, but also leads to large variance in the number of particles in the region and high entanglement of the order of the values seen for free fermions. These intermediate microemulsion metallic phases are embedded in an insulating phase. Further study of their properties is needed as well as their connection to the rare thermalizing inclusions postulated to drive the Griffiths phases close to the many-body localization transition [33,34], to phase separation in two-dimensional systems [32], and to the enhancement of the persistent current in rare disordered systems [31].

ACKNOWLEDGMENTS

Useful discussions with A. Turner and G. Murthy are gratefully acknowledged.

-
- [1] P. W. Anderson, *Phys. Rev.* **109**, 1492 (1958).
 - [2] J.-Y. Choi, S. Hild, J. Zeiher, P. Schauss, A. Rubio-Abadal, T. Yefsah, V. Khemani, D. A. Huse, I. Bloch, and C. Gross, *Science* **352**, 1547 (2016) and references therein.
 - [3] R. Stano and P. Jacquod, *Nat. Photonics* **7**, 66 (2013) and references therein.
 - [4] For a review, see P. A. Lee and T. V. Ramakrishnan, *Rev. Mod. Phys.* **57**, 287 (1985).
 - [5] D. Basko, I. Aleiner, and B. Altshuler, *Ann. Phys.* **321**, 1126 (2006).
 - [6] For a recent review, see R. Nandkishore and D. A. Huse, *Annu. Rev. Condens. Matter Phys.* **6**, 15 (2015).
 - [7] R. Berkovits, *Phys. Rev. Lett.* **108**, 176803 (2012).
 - [8] A. Zhao, R.-L. Chu, and S.-Q. Shen, *Phys. Rev. B* **87**, 205140 (2013).
 - [9] R. Berkovits, *Phys. Rev. B* **89**, 205137 (2014).
 - [10] H. Li and F. D. M. Haldane, *Phys. Rev. Lett.* **101**, 010504 (2008).
 - [11] N. Laflorencie, *Phys. Rep.* **646**, 1 (2016) and references therein.
 - [12] M. Koch-Janusz, K. Dhochak, and E. Berg, *Phys. Rev. B* **95**, 205110 (2017).
 - [13] V. Alba, M. Haque, and A. M. Läuchli, *Phys. Rev. Lett.* **108**, 227201 (2012).
 - [14] M. Serbyn, A. A. Michailidis, D. A. Abanin, and Z. Papić, *Phys. Rev. Lett.* **117**, 160601 (2016).
 - [15] R. A. Römer and M. Schreiber, *Phys. Rev. Lett.* **78**, 515 (1997).
 - [16] F. Woynarovich and H. P. Eckle, *J. Phys. A: Math. Gen.* **20**, L97 (1987); C. J. Hamer, G. R. W. Quispel, and M. T. Batchelor, *ibid.* **20**, 5677 (1987).
 - [17] T. Giamarchi, *Quantum Physics in One Dimension* (Oxford University Press, New York, 2003).
 - [18] W. Apel, *J. Phys. C: Solid State Phys.* **15**, 1973 (1982); W. Apel and T. M. Rice, *Phys. Rev. B* **26**, 7063 (1982).
 - [19] T. Giamarchi and H. J. Schulz, *Phys. Rev. B* **37**, 325 (1988).
 - [20] S. R. White, *Phys. Rev. Lett.* **69**, 2863 (1992); *Phys. Rev. B* **48**, 10345 (1993).
 - [21] U. Schollwöck, *Rev. Mod. Phys.* **77**, 259 (2005); K. A. Hallberg, *Adv. Phys.* **55**, 477 (2006).
 - [22] H. F. Song, S. Rachel, C. Flindt, I. Klich, N. Laflorencie, and K. Le Hur, *Phys. Rev. B* **85**, 035409 (2012).
 - [23] D. V. Averin and K. K. Likharev, *J. Low Temp. Phys.* **62**, 345 (1986).
 - [24] V. Khemani, F. Pollmann, and S. L. Sondhi, *Phys. Rev. Lett.* **116**, 247204 (2016).
 - [25] X. Yu, D. Pekker, and B. K. Clark, *Phys. Rev. Lett.* **118**, 017201 (2017).
 - [26] R. Berkovits, *Europhys. Lett.* **25**, 681 (1994); R. Berkovits and Y. Avishai, *J. Phys.: Condens. Matter* **8**, 389 (1996); R. Berkovits and B. I. Shklovskii, *ibid.* **11**, 779 (1999).
 - [27] S. D. Geraedts, R. Nandkishore, and N. Regnault, *Phys. Rev. B* **93**, 174202 (2016).

- [28] A. Wobst, G.-L. Ingold, P. Hänggi, and D. Weinmann, *Eur. Phys. J. B* **27**, 11 (2002).
- [29] I. Klich and L. Levitov, *Phys. Rev. Lett.* **102**, 100502 (2009).
- [30] B. Hsu, E. Grosfeld, and E. Fradkin, *Phys. Rev. B* **80**, 235412 (2009).
- [31] P. Schmitteckert, R. A. Jalabert, D. Weinmann, and J.-L. Pichard, *Phys. Rev. Lett.* **81**, 2308 (1998).
- [32] B. Spivak and S. A. Kivelson, *Phys. Rev. B* **70**, 155114 (2004); R. Jamei, S. Kivelson, and B. Spivak, *Phys. Rev. Lett.* **94**, 056805 (2005).
- [33] S. Gopalakrishnan, M. Muller, V. Khemani, M. Knap, E. Demler, and D. A. Huse, *Phys. Rev. B* **92**, 104202 (2015).
- [34] L. Zhang, B. Zhao, T. Devakul, and D. A. Huse, *Phys. Rev. B* **93**, 224201 (2016).